Journal of Constructional Steel Research 65 (2009) 497–508

Contents lists available at ScienceDirect

Journal of Constructional Steel Research

journal homepage: www.elsevier.com/locate/jcsr

Analytical behavior of frames with steel beams to concrete-filled steel tubular column

Wen-Da Wang [a,b], Lin-Hai Han [b,*], Xiao-Ling Zhao [c]

[a] College of Civil Engineering, Lanzhou University of Technology, Lanzhou, 730050, China
[b] Department of Civil Engineering, Tsinghua University, Beijing, 100084, China
[c] Department of Civil Engineering, Monash University, Clayton, VIC 3168, Australia

ARTICLE INFO

Article history:
Received 11 March 2008
Accepted 2 November 2008

Keywords:
Concrete filled steel tubes
Column
Steel beam
Composite frame
Failure mode
Hysteretic model

ABSTRACT

This paper reports the mechanism of composite frames with steel beams connected to concrete-filled square hollow section (SHS) columns. Detailed analysis was carried out on longitudinal stress in steel beams, axial stress distribution in concrete, and concrete stress along the column height and at the connection panel. Parametric studies were conducted to investigate the influence of axial load level, beam-to-column linear stiffness ratio on the structural behavior of composite frames. Simplified hysteretic lateral load (P) versus lateral displacement (Δ) models are proposed for such composite frames.

1. Introduction

Hollow structural steel (HSS) columns filled with concrete offer a number of benefits and are often used in tall buildings and other industrial structures. Concrete-filled steel tubular (CFST) columns are increasingly used in buildings due to their excellent static and seismic performance.

Chen et al. [1] presented different methods of advanced analysis for steel frames, such as elastic–plastic hinge method, refined plastic hinge method and plastic zone method. The analysis and design of composite frames with steel columns and steel–concrete composite beams under static loading were reported in Liew and Uy [2], Nethercot [3], Johnson [4], Li et al. [5,6]. The design of such composite frames under cyclic loading was reported in Plumier et al. [7], Bursi et al. [8], Thermou et al. [9]. CFST columns were not used in the above mentioned composite frames. Limited work was conducted on composite frames with CFST columns, as summarized in Hajjar [10] which also indicated the need to study mechanics models for such composite frames.

The authors have performed experimental investigation, as well as a finite element analysis (FEA) modeling on composite frames, consisting of steel beams and CFST columns [11]. This paper presents a detailed analysis on longitudinal stress in steel beams, axial stress distribution in concrete, and concrete stress along the column height and at the connection panel, by using the FEA modeling with ABAQUS [12]. Parametric studies are conducted to investigate the influence of axial load level and beam-to-column linear stiffness ratio on the structural behavior of composite frames. Simplified hysteretic lateral load (P) versus lateral displacement (Δ) models are proposed for such composite frames.

2. Stress analysis of the composite frame structures

2.1. General

A series of tests and FEA model on composite frames with steel beam to concrete-filled SHS steel tubular columns were conducted by the authors [11]. A typical frame specimen SF-22 [11] was selected to illustrate the mechanic model of the composite frames. The column in frame SF-22 is a concrete-filled SHS with a width of 140 mm and a thickness of 4 mm. The beam in frame SF-22 is an I-section with a flange width of 80 mm, a web depth of 180 mm and a thickness of 4.34 mm. In order to describe various stress distribution and deformation of the frames, five load stages were marked in the lateral load (P) versus lateral displacement (Δ) curves of the composite frame, as shown in Fig. 1.

The five points in Fig. 1 represent different stages during the incremental lateral load. Point one corresponds to the stage when the extreme fibers of the steel beam start to yield. Point two refers to the stage when the compression fibers of CFST steel columns reach their yield stress. Point three shows the ultimate lateral

* Corresponding author. Tel.: +86 10 62797067; fax: +86 10 62781488.
E-mail address: lhhan@tsinghua.edu.cn (L.-H. Han).

0143-974X/$ – see front matter © 2008 Elsevier Ltd. All rights reserved.
doi:10.1016/j.jcsr.2008.11.002

Nomenclature

E_c	Modulus of elasticity of concrete
E_s	Modulus of elasticity of steel
EI_c	Stiffness of CFST column
f'_c	Concrete cylinder compressive strength
f_t	Concrete tension strength
f_y	Yield strength of steel
i_b	Linear stiffness of steel beam for composite frame ($i_b = E_s I_b/L$)
i_c	Linear stiffness of CFST column for composite frame ($i_c = EI_c/L_c$)
I_b	Moment of inertia for steel beam
I_c	Moment of inertia for core concrete cross section
I_s	Moment of inertia for hollow steel cross section
k	Beam–column linear stiffness ratio
K_a	Stiffness in the elastic stage of composite frame for hysteretic model
K_T	Stiffness of the descending stage of composite frame for hysteretic model
k_m	Ultimate moment ratio between steel beam and CFST column of composite frame
L	The length of steel beam
L_c	Height of CFST column
M_{pc}	Ultimate moment of CFST column
n	Axial load level ($n = N/N_u$)
N	Axial load of CFST column
N_u	Ultimate compression resistance of CFST column
p	The hardening stage coefficient of moment versus curvature model for CFST column
P	Lateral load of frame
P_y	Ultimate lateral load capacity of composite frame in the hysteretic model
P_{yc}	Ultimate lateral load capacity of CFST column of composite frame in the hysteretic model
P_{max}	Ultimate lateral load capacity of frame
P_{ua}	Ultimate lateral load capacity of frame by ABAQUS
α	Steel ratio ($\alpha = A_s/A_c$)
σ	Stress
ε	Strain
Δ	Lateral displacement of frame
Δ_p	Lateral displacement when lateral load reaches P_y in the hysteretic model
Δ_u	Lateral displacement when lateral load of frame falls 85% of P_{max}
Δ_y	Yield displacement of frame
μ	Displacement ductility coefficient
μ_L	Effective length coefficient of CFST column

load (P_{max}) of the composite frame. Point four corresponds to the stage when the deflection reaches twice Δ_{max}. Point five is the stage when the load reaches 85% of the ultimate load P_{max}. Several sections in CFST columns and steel beam are selected (see Fig. 2) for stress analysis. Sections B1 and B2 are the plastic hinge locations in steel beam. Sections C1 and C2 are located at the bottom and top of the left CFST column. Section C1 is located near and outside of the stiffeners of columns, and section C2 is located under the steel beam. Sections C3 and C4 are the same as sections C1 and C2 except that they are located in the right column. Sections C5 and C6 are at the middle section of the left and right CFST column respectively, as shown in Fig. 2(a). Fig. 2(b) shows the deformation of the composite frame SF-22 at failure load. The four plastic hinges were located at the sections B1 and B2 in the steel beam and at sections C1 and C3 in the CFST columns. The deformation

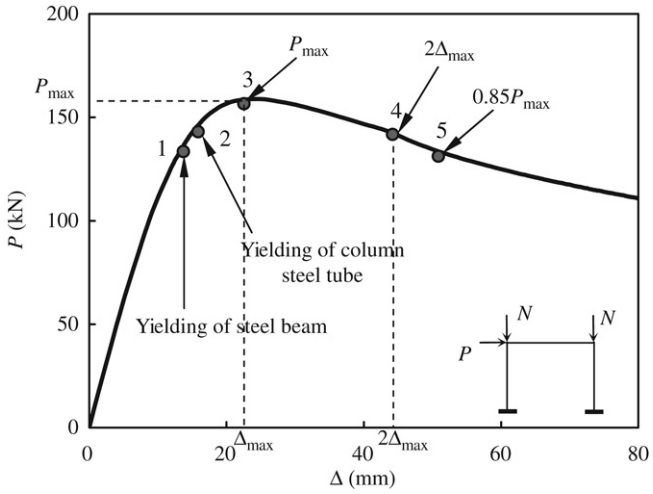

Fig. 1. Lateral load (P) versus displacement (Δ) curves of typical CFST frame SF-22 (Five Stages).

of the four plastic hinge sections at stage five, defined in Fig. 1, are shown in Fig. 3(a)–(d), respectively. The steel tubes of CFST columns at section C1 and C3 show evident outward buckling, whereas obvious local buckling occurs in the flanges and web of beam at section B1 and B2. The experimental result and FEA result by ABAQUS are consistent, as shown in Fig. 3.

2.2. Longitudinal stress in steel beams

Fig. 4 shows the longitudinal stress distribution of the steel beam of specimen SF-22 during the various load stages (e.g. one, three and five as defined in Fig. 1). The longitudinal tension and compression stress of section B1 and B2 were described as shown in Fig. 4(a)–(f). There was slight difference between the left beam end (B1) and the right beam end (B2). The beam was separated into two parts by a bending inflexion, and the two parts of the beam had different deformation curves. The inflexion was located approximately at the middle of the beam. The left part of the beam (B1) was in compression in the top flange and the upper web, and in tension in the bottom flange and the lower web. The right part of beam (B2) had the opposite sign. The plastic hinges were located near the ring plate. The compression and tension stress of steel beam were increasing with the incremental lateral load. The compression stress of flange at section B2 reached the yield stress. The yield area had extended from flange to web. When the composite frame reached its ultimate load (Stage three), about half of compression web in section B2 yielded. The tension area of web at section B2 did not yield at this stage. The lateral load began to descend from stage three, and local buckling appeared on the compressive web at section B2. The stress and deformation at section B1 were similar to section B2, but the stress value in section B1 was less than that in section B2, where the deformation of section B1 was smaller than that of section B2.

2.3. Concrete axial stress distribution

Fig. 5 shows the concrete axial stress distribution of section C1 of the composite frame SF-22 at the typical five load stages. f'_c is the cylinder compression strength of the concrete in the isoline. From Fig. 5, the axial stresses of concrete are different at various load stages. The section of CFST columns were compressed before the lateral load was applied. The tension area of the CFST square section appeared with the increasing of the lateral load. The tension area in concrete in CFST SHS columns extended, and the compression area decreased, with the incremental lateral